Article

Cell Stem Cell

Transient Pairing of Homologous *Oct4* Alleles Accompanies the Onset of Embryonic Stem Cell Differentiation

Graphical Abstract

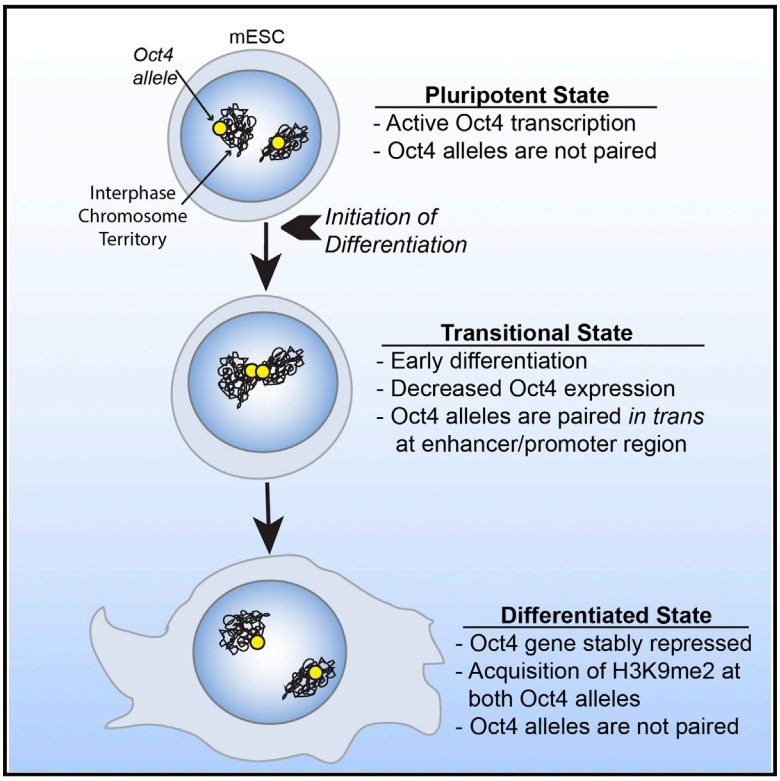

Highlights

- Homologous alleles of the Oct4 gene transiently associate as ESCs exit pluripotency
- Onset of Oct4 allelic pairing is determined by the kinetics of ESC differentiation
- The 5′ regulatory region of Oct4 is necessary and sufficient for allelic pairing
- OCT4/SOX2 binding motifs are critical mediators of homologous allele pairing

Authors

Megan S. Hogan, David-Emlyn Parfitt, ..., Michael M. Shen, David L. Spector

Correspondence

spector@cshl.edu

In Brief

Hogan et al. describe association of the Oct4 alleles at the onset of ESC differentiation. These inter-chromosomal interactions are mediated by OCT4/SOX2 binding motifs within the promoter/enhancer region of the *Oct4* gene, suggesting a transvection-like mechanism that influences gene regulation at the *Oct4* locus.

Accession Numbers

GSE65510

Hogan et al., 2015, Cell Stem Cell *16*, 275–288
March 5, 2015
http://dx.doi.org/10.1016/j.stem.2015.02.001

Cell Stem Cell
Article

Transient Pairing of Homologous *Oct4* Alleles Accompanies the Onset of Embryonic Stem Cell Differentiation

Megan S. Hogan,[1,3] David-Emlyn Parfitt,[2,4] Cinthya J. Zepeda-Mendoza,[1] Michael M. Shen,[2] and David L. Spector[1,*]
[1]Cold Spring Harbor Laboratory, Watson School of Biological Sciences, One Bungtown Road, Cold Spring Harbor, NY 11724, USA
[2]Departments of Medicine and Genetics & Development, Columbia University Medical Center, New York, NY 10032, USA
[3]Present address: Icahn School of Medicine at Mount Sinai, Black Family Stem Cell Institute, 1 Gustave L. Levy Place, New York, NY 10029, USA
[4]Present address: Celmatix Incorporated, 54 West 40th Street, New York, NY 10018, USA
*Correspondence: spector@cshl.edu
http://dx.doi.org/10.1016/j.stem.2015.02.001

SUMMARY

The relationship between chromatin organization and transcriptional regulation is an area of intense investigation. We characterized the spatial relationships between alleles of the *Oct4*, *Sox2*, and *Nanog* genes in single cells during the earliest stages of mouse embryonic stem cell (ESC) differentiation and during embryonic development. We describe homologous pairing of the *Oct4* alleles during ESC differentiation and embryogenesis, and we present evidence that pairing is correlated with the kinetics of ESC differentiation. Importantly, we identify critical DNA elements within the *Oct4* promoter/enhancer region that mediate pairing of *Oct4* alleles. Finally, we show that mutation of OCT4/SOX2 binding sites within this region abolishes inter-chromosomal interactions and affects accumulation of the repressive H3K9me2 modification at the *Oct4* enhancer. Our findings demonstrate that chromatin organization and transcriptional programs are intimately connected in ESCs and that the dynamic positioning of the *Oct4* alleles is associated with the transition from pluripotency to lineage specification.

INTRODUCTION

The spatial organization of chromatin within the cell nucleus contributes toward the overall mechanism by which gene expression and repression is regulated (reviewed in Hübner et al., 2013; Joffe et al., 2010). In somatic cells, the genome is spatially segregated into active and inactive chromosomal regions (Lieberman-Aiden et al., 2009; Nagano et al., 2013; Simonis et al., 2006) and further subdivided into evolutionarily conserved topologically associated domains (Dixon et al., 2012; Nora et al., 2012). Emerging evidence also indicates that cell-type-specific chromatin organization exists at the sub-megabase level (Phillips-Cremins et al., 2013; Whyte et al., 2013; Zhang et al., 2013). Interestingly, the differences in chromatin organization between distinct cell types correlate with differences in their transcriptional programs (reviewed in Duan and Blau, 2012).

Although the transcriptional and epigenetic landscape of embryonic stem cells (ESCs) has been extensively characterized (reviewed in Young, 2011), the impact of nuclear organization and chromatin dynamics on the regulation of ESC pluripotency and differentiation has been less well established. Previous studies have demonstrated a dramatic re-organization of nuclear architecture that occurs during ESC differentiation, as highlighted by several microscopic studies (Aoto et al., 2006; Eckersley-Maslin et al., 2013; Kobayakawa et al., 2007; Melcer et al., 2012; Meshorer and Misteli, 2006) and by genome-wide mapping of lamina-associated domains (Peric-Hupkes et al., 2010). Interestingly, recent chromosome conformation capture-based studies revealed that intra- and inter-chromosomal interactions between genomic regions also differ between ESCs and other cell types, and that these differences correlate with cell-type-specific gene expression (Apostolou et al., 2013; de Wit et al., 2013; Denholtz et al., 2013; Kagey et al., 2010; Nora et al., 2012; Phillips-Cremins et al., 2013; Wei et al., 2013; Zhang et al., 2013). Although these studies have provided an understanding of the differences in chromatin interaction frequencies before and after ESC differentiation, the dynamic nuclear landscape that exists in single cells during the loss of ESC pluripotency and the onset of differentiation has not been examined.

In this study, we characterized the spatial relationships between alleles of the *Oct4*, *Sox2*, and *Nanog* genes in single cells during the earliest stages of mouse ESC differentiation and embryonic development. Using multi-color DNA fluorescence in situ hybridization (FISH) and 3D analysis of gene position in individual nuclei, we describe for the first time homologous pairing of the *Oct4* alleles, and present evidence that such homologous pairing is correlated with the kinetics of ESC differentiation. Further, we observe *Oct4* allelic pairing throughout the ectoderm/neuroectoderm of E7.75 mouse embryos, a developmental stage when dynamic regulation of *Oct4* and lineage specification occurs in vivo. Importantly, we identify critical DNA elements within the *Oct4* promoter/enhancer region that are sufficient to mediate inter-chromosomal interactions of a transgene with endogenous *Oct4* alleles. Finally, we show that mutation of OCT4/SOX2 binding sites within this critical pairing region abolishes inter-chromosomal interactions and disrupts the accumulation of repressive epigenetic modifications at the *Oct4* enhancer. Our

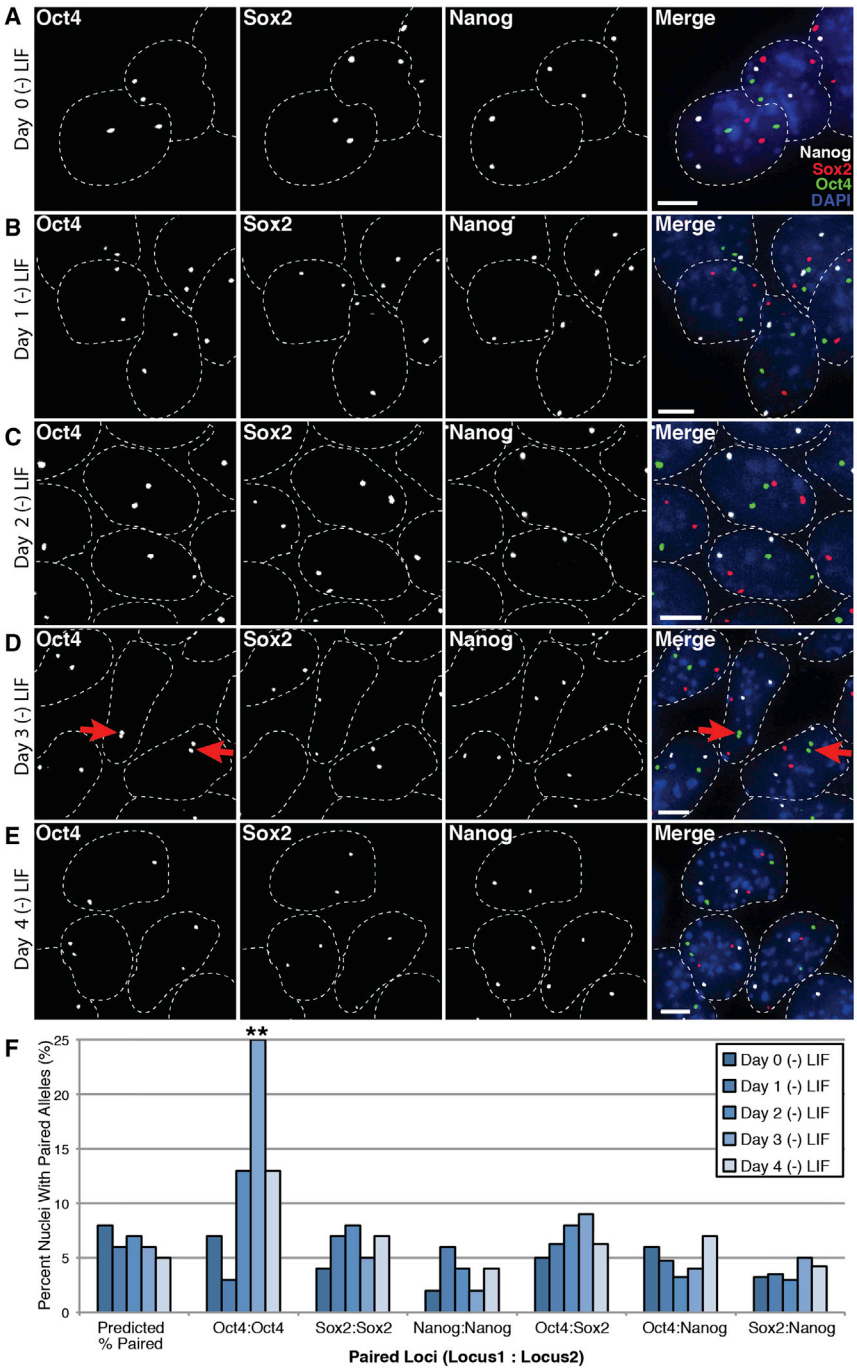

Figure 1. Assessing Potential Homologous and Heterologous Interactions between *Oct4*, *Sox2*, and *Nanog* Gene Loci during ESC Differentiation

(A–E) Representative images of 3D multi-color DNA FISH analysis of gene position in ESCs, at 0, 1, 2, 3, and 4 days after the withdrawal of LIF. Individual ESC nuclei outlined with dashed line. Red arrows in (D) denote paired *Oct4* alleles. Scale bar represents 5 μm.

(F) Quantification of allelic interactions among *Oct4*, *Sox2*, and *Nanog* alleles. n = 100 per locus pair at each time point. The p values for the two-sample z-test statistic are reported. **$p < 0.01$. See also Figures S1 and S2.

findings demonstrate that chromatin organization and transcriptional programs are connected in ESCs, and that the dynamic positioning of the *Oct4* alleles that occurs during ESC differentiation is linked to an exit from the pluripotent state.

RESULTS

Characterization of the Nuclear Position of Pluripotency Regulators during ESC Differentiation

Because transcriptional regulation of *Oct4*, *Sox2*, and *Nanog* genes is critical to the transition between pluripotency and lineage specification, we were interested in examining their nuclear organization during early ESC differentiation. The *Oct4*, *Sox2*, and *Nanog* genes are co-regulated, being bound by similar transcription factors (Boyer et al., 2005; Loh et al., 2006). Given the evidence that some co-regulated genes may spatially cluster together in other cell types (Brown et al., 2008; Kosak et al., 2007; Papantonis et al., 2012; Schoenfelder et al., 2010), we sought to determine whether *Oct4*, *Sox2*, and *Nanog* gene loci were spatially clustered in ESCs, and whether the spatial relationship between these gene loci changed during ESC differentiation.

To assess the dynamic spatial relationship between *Oct4*, *Sox2*, and *Nanog* gene loci during ESC differentiation, v6.5 mouse ESCs were grown on coverslips in medium without leukemia inhibitory factor (LIF), and allowed to differentiate for four days. These ESCs were then fixed at 0, 1, 2, 3, and 4 days (−)LIF and multi-color DNA FISH was performed using DNA probes to *Oct4*, *Sox2*, and *Nanog* gene loci (Figures 1A–1E). Distances between DNA FISH signals in individual nuclei were measured in 3D, and in accordance with previous studies of inter-chromosomal associations (Augui et al., 2007; Bacher et al., 2006; Hewitt et al., 2009; Lasalle and Lalande, 1996; Masui et al., 2011), gene loci that were separated by a 3D distance of less than 2 μm were classified as "paired" or "associated."

The distance between homologous and heterologous gene loci was measured at each time point during differentiation, and the percentage of nuclei with paired homologous or heterologous gene alleles was assessed (Figure 1F, see also Figures S1 and S2). Analysis of the frequency of allelic associations revealed that co-regulated *Oct4*, *Sox2*, and *Nanog* loci do not cluster together in undifferentiated ESCs. However, when differentiating ESCs were examined, we found that the homologous alleles of

the *Oct4* gene associate with each other with increased frequency at Day 3 (−)LIF (Figures 1D and 1F). The observed association of homologous *Oct4* alleles during ESC differentiation was particularly intriguing, because pairing of homologous chromosomes is not a general feature of mammalian somatic cells (Duncan, 2002). Therefore, the occurrence of homologous *Oct4* allelic associations was investigated in further detail.

Homologous Allelic Pairing during ESC Differentiation Is Specific to the *Oct4* Locus

To investigate whether somatic homolog associations were a pervasive phenomenon during ESC differentiation, we measured the frequency of homologous allelic associations at additional gene loci by DNA FISH in undifferentiated ESCs (Day 0), and ESCs cultured for 3 days without LIF. Association of the *Oct4* alleles was again observed at Day 3 (−)LIF, but not at Day 0 (Figure 2A). Interestingly, only the *Oct4* locus showed a significant level of allelic associations at Day 3 (−)LIF; whereas other pluripotency gene loci (*Sox2*, *Nanog*), housekeeping gene loci (β-*actin, Col1A1*), distal regions of mouse chromosome 17 (C17E3), and the many other genomic regions examined (Table S1 and data not shown) failed to show a significant level of allelic associations during ESC differentiation (Figure 2A). Thus, the allelic pairing observed at Day 3 (−)LIF is not a general feature of all gene loci in differentiating ESCs, but rather an event specific to the *Oct4* gene locus.

The Timing of *Oct4* Allelic Pairing Reflects the Kinetics of ESC Differentiation

Although numerous studies have shown a relationship between nuclear organization and transcription, the specific mechanism(s) by which a gene's position may affect gene expression remain unclear. Therefore, we sought to investigate whether *Oct4* allelic pairing might be involved in the transcriptional regulation of the *Oct4* gene as differentiation proceeds. To assess the transcriptional status of paired *Oct4* alleles in individual nuclei, Oct4 RNA FISH was performed in combination with *Oct4* DNA FISH on ESCs at Day 3 (−)LIF. This analysis revealed that 37% of paired *Oct4* alleles show transcription from both alleles (Figure 2B, upper), 24% show transcription from only one allele (Figure 2B, middle), whereas 39% show no visible transcripts at either allele (Figure 2B, bottom). These results suggest that allelic associations may commence prior to or concurrent with the repression of the *Oct4* gene as differentiation progresses. Alternatively, *Oct4* allelic pairing may be coincident with increased transcriptional pulsing at the locus and modulation of *Oct4* expression levels. Importantly, RNA FISH signals were not detected at either *Oct4* allele after 5 days (−)LIF (data not shown), confirming that both copies of the gene are repressed during ESC differentiation. Therefore, *Oct4* allelic pairing occurs during the transition of *Oct4* expression from an "on" to "off" state.

Next, we tested whether varied differentiation paradigms might affect the timing and/or frequency of *Oct4* allelic associations. To this end, we used an ESC line containing a stably integrated DOX-inducible shRNA to *Oct4* (Oct4.468/R26-rtTA ESCs) (Premsrirut et al., 2011), and induced differentiation using three distinct paradigms: (−) LIF, addition of retinoic acid (RA), and DOX-induced *Oct4* shRNA expression (Figure 2C). Interestingly, RT-qPCR analysis of *Oct4* gene expression revealed that the kinetics of *Oct4* gene repression varied depending on the differentiation protocol used (Figure 2D). LIF withdrawal induced a gradual decrease in *Oct4* expression over the course of the 3 days; *Oct4* mRNA levels were reduced to less than 50% of Day 0 expression levels by Day 3 (−)LIF (Figure 2D). In contrast, treatment with RA or Oct4 shRNA resulted in a more rapid loss of *Oct4* gene expression; transcript levels were reduced to 40% and 20% of Day 0 expression levels, respectively, after just 1 day of differentiation (Figure 2D).

When *Oct4* allelic pairing was assessed, the onset of pairing was again observed at Day 3 (−)LIF, coincident with the downregulation of *Oct4* gene expression (Figures 2E and 2F). In contrast, ESCs differentiated with RA or *Oct4* shRNA induction showed an earlier onset of *Oct4* allelic associations, after only 1 day of differentiation (Figures 2E and 2F). Remarkably, the earlier onset of *Oct4* allelic pairing observed with RA or shRNA treatment is accompanied by a more rapid loss of *Oct4* gene expression in these differentiation paradigms. Thus, the timing of *Oct4* allelic pairing corresponds to the kinetics of *Oct4* gene repression in each differentiation paradigm. These results suggest that the pairing of *Oct4* alleles is associated with *Oct4* gene repression, or is linked to a particular developmental stage in which *Oct4* downregulation occurs.

Homologous Pairing of *Oct4* Alleles Occurs during Early Embryonic Development

Although differentiating ESCs can partially recapitulate embryonic development in vitro, we were interested in whether the observed *Oct4* allelic associations would also occur in vivo during early mouse embryo development. In the post-implantation mouse epiblast, *Oct4* expression in the ectoderm/neuroectoderm is downregulated in an anterior to posterior manner concurrent with neural lineage specification and loss of pluripotency (Downs, 2008; Lupu et al., 2008; Osorno et al., 2012). We reasoned that if *Oct4* allelic pairing was correlated with repression of the *Oct4* gene, high levels of *Oct4* allelic pairing should be observed in nuclei of the anterior neuroectoderm where the gene was being coordinately repressed. Thus, we assessed the frequency of *Oct4* allelic association in sagittal sections of late head fold stage (Downs and Davies, 1993) mouse embryos, which were harvested at E7.75. Embryos were immunolabeled with an OCT4 antibody to identify regions of the embryo actively expressing the OCT4 protein (Figures 3A–3C), and immunostaining was assessed in three embryonic regions as indicated: anterior (*Ant.*), middle (*Mid.*), and posterior (*Pos.*) (Figures 3A and S3). Next, multicolor DNA FISH was performed, using DNA probes to *Oct4*, *Sox2*, and *Nanog* gene loci. Distances between homologous alleles were measured in ectoderm/neuroectoderm cells, and the percentage of nuclei with paired homologous loci was calculated for each embryonic region (Figures 3D–3G). Interestingly, pairing of homologous *Oct4* alleles was observed at roughly equal levels (~25%–30%) in ectoderm/neuroectoderm cells of all three regions, regardless of the level of OCT4 immunofluorescence observed in each region (Figures 3D–3G). When distances between *Nanog* and *Sox2* alleles were assessed in the same nuclei, allelic associations were not observed (Figure 3G). In addition, examination of distances between *Oct4* alleles in embryos at earlier (approximately embryonic day 6.5 [E6.5], epiblast cells) and later (~E9.5, neural epithelium) stages

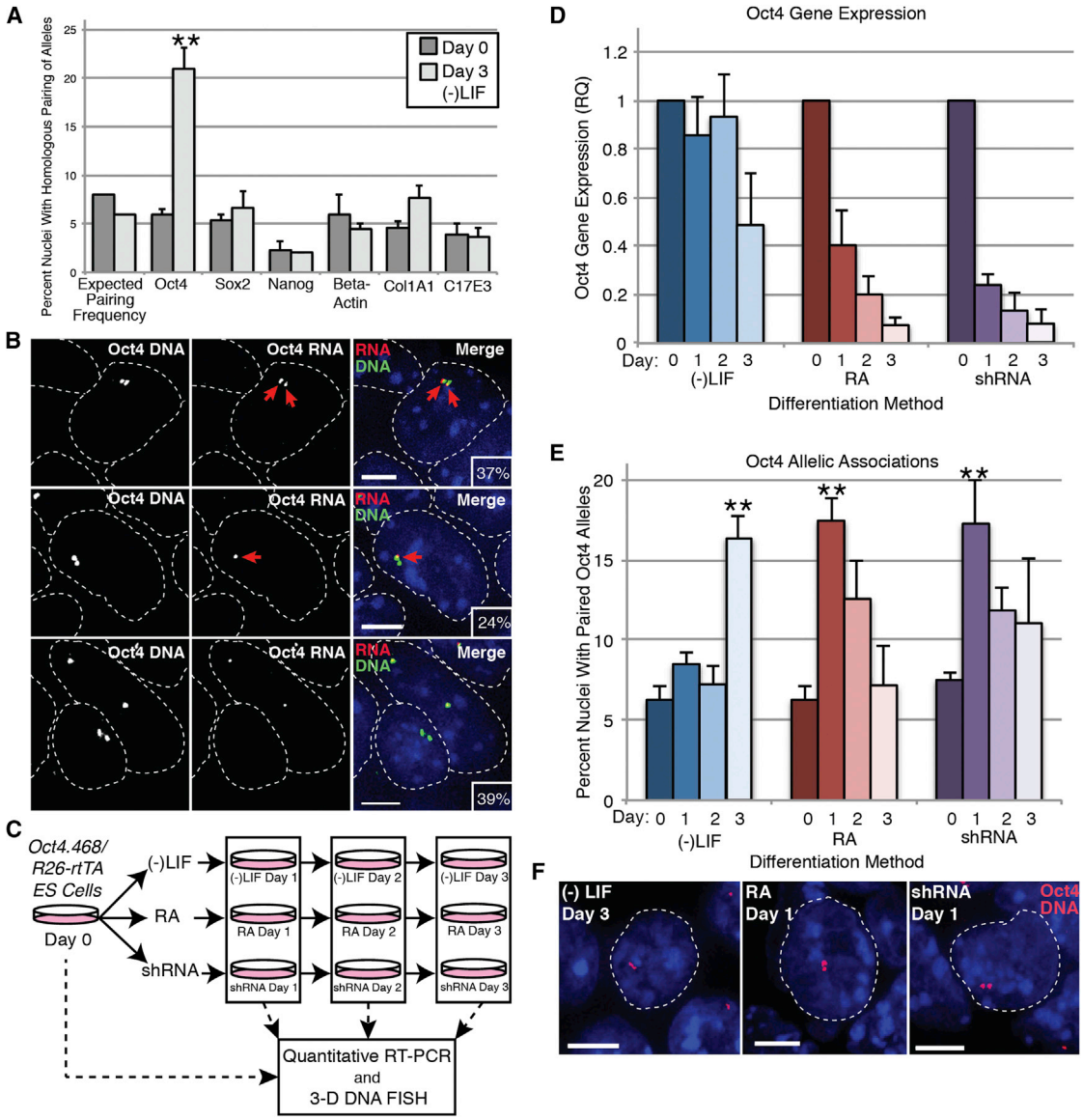

Figure 2. The Timing of *Oct4* Allelic Pairing Reflects the Kinetics of ESC Differentiation

(A) Quantification of homologous pairing at representative genomic loci in ESCs before (Day 0) and after 3 days of differentiation (−)LIF. n = 100 per locus pair at each time point, error bars represent ± SEM of three biological replicates. **p < 0.01.

(B) Assessment of the transcriptional status of paired *Oct4* alleles, by RNA and DNA FISH. The percentage of paired *Oct4* alleles with two active alleles (top, red arrows), one active allele (middle, red arrow), or zero active alleles (bottom) is indicated. Individual ESC nuclei are outlined with a dashed line. n = 93 paired loci. Scale bar represents 5 μm.

(C) Schematic diagram of differentiation scheme with Oct4.468/R26-rtTA ESCs.

(D) Assessment of *Oct4* gene expression by quantitative RT-PCR over 3 days of differentiation, using (−)LIF, RA, or shRNA differentiation paradigms. Gene expression is normalized to β-actin expression for each sample.

(E) Quantification of *Oct4* allelic interactions over 3 days of differentiation, using (−)LIF, RA, or shRNA differentiation paradigms. n = 100 for each time point. Error bars represent ± SEM of three biological replicates. The p values for the two-sample z-test statistic are reported. **p < 0.01.

(F) Representative images of paired Oct4 alleles in Oct4.468/R26-rtTA ESCs differentiated in (−)LIF, RA, or shRNA conditions. Scale bar represents 5 mm.

See also Tables S1 and S2.

of development did not show a significant level of allelic associations compared to control loci (Figures S3D–S3F). These results are consistent with our in situ data and indicate that the pairing of *Oct4* alleles is linked to a developmental time point when expression of the *Oct4* gene is being regulated.

The 5′ Regulatory Region of the *Oct4* Gene Mediates Inter-Chromosomal Associations at the *Oct4* Locus

Having observed that allelic pairing of the *Oct4* gene is associated with the transition from pluripotency to differentiation, we sought to elucidate the mechanism facilitating pairing of the

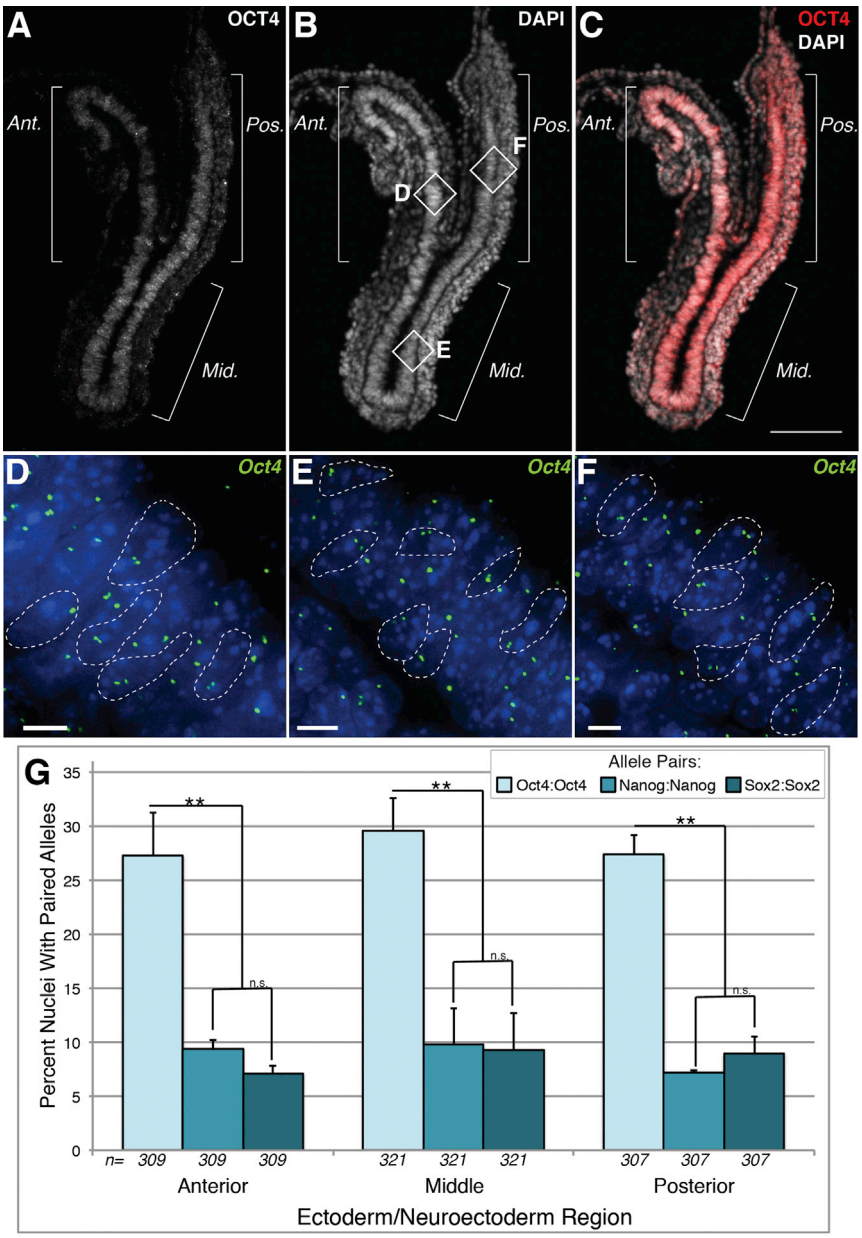

Figure 3. *Oct4* Allelic Associations Occur during Post-Implantation Development In Vivo

(A–C) Representative images of a 10 μm sagittal cryosection of an E7.75 mouse embryo, showing (A) OCT4 immunofluoresence (IF), (B) DAPI-stained nuclei, and (C) OCT4 IF overlaid with DAPI. Scale bar represents 100 μm.

(D–F) Enlargement of corresponding boxed areas in (B), showing *Oct4* DNA FISH in the (D) anterior, (E) middle, and (F) posterior regions of the ectoderm/neuroectoderm. Nuclei with paired *Oct4* alleles are outlined with dashed lines. Scale bar represents 5 μm.

(G) Quantification of allelic associations in E7.75 embryos. Error bars represent ± SEM of three biological replicates. The p values for the two-sample z-test statistic are reported. **$p < 0.01$.

See also Figure S3.

Oct4 alleles. We reasoned that specific protein and/or RNA factors bind to the *Oct4* locus and mediate the pairing event, and that the *Oct4* locus must therefore contain specific DNA elements where such factors will bind. To assess the role of the genomic DNA sequence in *Oct4* allelic pairing, ESC lines with single-copy, site-specific integrations of various fragments of a 10kb region of genomic DNA surrounding and including the *Oct4* gene were generated.

A schematic diagram of the strategy used for targeted insertion of *Oct4* fragments at the *Col1A1* locus in KH2 ESCs (Beard et al., 2006) is shown in Figure 4A. The 10kb *Oct4* genomic region of interest was divided into four fragments (Figure 4B), and four new ESC lines (OCF2, OCF3, OCF4, and OCF5) were generated via Flp-mediated recombination. Transgene-specific DNA FISH probes were used to verify proper transgene integration at the *Col1A1* locus in resulting ESC clones (Figure 4C). Next, each new ESC line was differentiated with RA for 1 day, and the frequency of transgene associations with the endogenous *Oct4* alleles was assessed.

To compare the contribution of the transgenic fragment to the pairing event, the following 3D distance measurements were made in each ESC nucleus: the distance between endogenous *Oct4* alleles (Oct4(En): Oct4(En), Figures S4B and 4D, arrow 1), the distance from the WT-*Col1A1* locus to each endogenous *Oct4* allele (WT-Col1A: Oct4(En), Figures S4A and 4D, arrow 2), and the distance from the Tg-*Col1A1* locus to the nearest endogenous *Oct4* allele (Tg-Col1A: Oct4(En), Figures S4C and 4D, arrow 3). For each of the ESC lines tested, the endogenous alleles of the *Oct4* gene paired with significant frequency at Day 1 of RA differentiation, as expected (Figures 4E and S4B). Furthermore, WT-*Col1A1* and endogenous *Oct4* alleles did not associate to a significant degree on Day 1 of RA differentiation in any of the tested ESC lines (Figures 4E and S4A). Strikingly, when the frequency of Tg-*Col1A1* and endogenous *Oct4* alleles was assessed in each cell line, the OCF2 transgenic allele showed an increased frequency of Oct4(En) associations compared to WT-*Col1A1* (Figures 4E and S4C). In OCF2 ESC nuclei where these associations were observed, interactions between the OCF2 transgene and endogenous *Oct4* loci involved one Oct4 allele in 83% of nuclei (Figure 4F), and both endogenous *Oct4* alleles in 17% of nuclei (Figure 4G). These results suggest that DNA elements exist within the OCF2 DNA fragment that are sufficient to mediate pairing of a transgenic locus with endogenous *Oct4* loci.

OCT4 Protein Binding Sites within the OCF2 DNA Fragment Are Necessary for *Oct4* Allelic Associations

The OCF2 DNA fragment contains 3.6 kb of genomic DNA sequence from the 5′ regulatory region of the *Oct4* gene, which includes the distal enhancer (DE), proximal enhancer, and a fragment of the *Oct4* promoter (ΔPr, Figure 5A). Although this 3.6 kb OCF2 fragment was sufficient to mediate pairing between the transgene and endogenous *Oct4* genes, we found that any further truncation of the 3.6 kb fragment abolished pairing activity (Figures S4D and S4E). Therefore, we reasoned that there may be multiple separate DNA elements/motifs along this 3.6 kb stretch of DNA, and that proteins binding to multiple sites in the 3.6 kb sequence may work synergistically to mediate allelic associations. Based on previously reported evidence of protein factors involved in somatic homolog pairing (Chaumeil and Skok, 2012; Donohoe et al., 2009; Ebert et al., 2011), we investigated CTCF, YY1, OCT4, and E2A proteins as candidates for a possible role in mediating *Oct4* allelic associations. To interrogate the importance of each of these proteins at the *Oct4* locus in a more specific manner, putative protein binding sites in the OCF2 DNA element were identified. Bioinformatic analysis revealed four potential OCT4 binding sites, six potential CTCF binding sites, seven potential YY1 binding sites, and eight potential E2A binding sites (Figure 5A). Because the OCT4 protein often binds as a heterodimer with SOX2 in ESCs (Young, 2011), the bioinformatically identified OCT4 binding sites were extended to encompass any adjacent SOX2 binding motifs, and these sites are therefore referred to as OCT4/SOX2 binding sites hereafter. Site-directed mutagenesis was performed with the pOCF2 plasmid as template, such that mutagenized targeting constructs had putative binding sites either for CTCF, YY1, OCT4/SOX2, and E2A replaced with scrambled DNA sequences (Table S3). The mutated OCF2 vectors were again used for site-specific integration at the *Col1A1* locus in KH2 ESCs, as detailed in Figure 4A, and ESC clones were analyzed by DNA FISH to verify targeted insertion of the transgene at the *Col1A1* locus (Figure 5B). The resulting four new ESC lines, OCF2ΔOCT4/SOX2, OCF2ΔCTCF, OCF2ΔYY1, and OCF2ΔE2A, were differentiated in RA medium for 1 day, and the frequency of transgene associations with the endogenous *Oct4* locus was assessed as described above. Endogenous *Oct4* alleles associated with each other to a significant degree in all of the ESC lines examined, as expected (Figure 5C). Mutagenesis of CTCF, E2A, and YY1 binding sites within the OCF2 fragment had only a weak effect on allelic associations (Figures 5C–5I). Remarkably, mutation of the OCT4/SOX2 binding sites in the OCF2 fragment produced a more dramatic effect. The *Tg-Col1A* locus in OCF2-ΔOCT4/SOX2 ESCs was not able to associate with the endogenous *Oct4* alleles to a significant degree (Figure 5C), indicating that the wild-type (WT) OCT4 binding sites are necessary to allow the OCF2 transgene to pair with endogenous *Oct4* loci. These results suggest that the OCT4 protein, or an OCT4 binding partner, may mediate the allelic associations observed during ESC differentiation.

Because mutations to the putative OCT4/SOX2 binding sites in the OCF2 fragment (Figure 6A) abrogated pairing between the transgene and endogenous *Oct4* alleles, we sought to verify that such mutations could truly disrupt OCT4 protein binding at these sequences using electrophoretic mobility shift assay. OCT4 protein was found to bind all four WT putative binding sites in vitro, as evidenced by the gel-shift (indicated by *→) in lanes containing OCT4 protein (Figure 6B, lanes 2, 8, 14, 20). Furthermore, in lanes containing mutated oligos, the shift produced by the addition of OCT4 protein was greatly diminished or completely absent (Figure 6B, lanes 5, 11, 17, 23). The loss of gel shift with the mutated oligos indicates that mutations to putative OCT4/SOX2 binding sites 1, 2, 3, and 4 disrupted OCT4 binding to these oligonucleotides in vitro.

To confirm that mutation of the OCT4 binding sites in the OCF2 region also disrupted OCT4 protein binding in situ, OCT4 chromatin immunoprecipitation (ChIP) was performed during ESC differentiation in both OCF2ΔOCT4/SOX2 ESCs and OCF2ΔYY1 ESCs. OCT4 occupancy was assayed by qPCR at 0, 3, and 6 days (−)LIF, using allele-specific Taqman probes to distinguish between WT and transgenic *Oct4* alleles. As shown in Figure 6C, mutation of the OCT4/SOX2 binding site on the *OCF2ΔOCT4/SOX2* allele leads to a significant decrease in OCT4 enrichment compared to the WT *Oct4* allele. In contrast, OCT4 enrichment at the *OCF2ΔYY1* allele is comparable to that of the WT *Oct4* allele (Figure 6D). These results indicate that pairing-competent alleles such as *OCF2ΔYY1* are bound by OCT4 in situ, but pairing-deficient alleles such as *OCF2ΔOCT4/SOX2* are not. Thus, these data are consistent with a role for the OCT4 protein in mediating allelic associations between the OCF2 transgene and endogenous *Oct4* alleles in situ.

Intact OCT4/SOX2 Binding Sites Are Necessary for Inter-Chromosomal Interactions and Coordination of H3K9me2 Modification during ESC Differentiation

To assess the role of OCT4/SOX2 binding sites at the molecular level, circular chromosome conformation capture followed by paired-end DNA sequencing (PE-4Cseq) was performed in pairing-deficient OCF2ΔOCT4/SOX2 ESCs and pairing-competent OCF2ΔYY1 ESCs before and after the onset of differentiation. Using the transgenic OCF2 region on chromosome 11 as bait, 4C templates were prepared from OCF2ΔOCT4/SOX2 ESCs (Figure 7A) and OCF2ΔYY1 ESCs (Figure 7B) after 0 or 3 days of differentiation (−)LIF. After paired-end sequencing, the frequency of inter-chromosomal interactions between the transgenic *OCF2* locus and the endogenous (WT) *Oct4* locus was assessed at each time point. Consistent with our DNA FISH data (Figure 5), PE-4Cseq revealed minimal *trans*-interactions between the WT *Oct4* locus and the *OCF2ΔOCT4/SOX2* transgene at both Day 0 and Day 3 (Figure 7C). However, the *OCF2ΔYY1* allele, which contains intact OCT4 protein binding sites, shows a significant increase in inter-chromosomal contact with the WT *Oct4* locus at Day 3 of ESC differentiation (Figure 7C). No significant differential intra-chromosomal interactions were identified using the FourCSeq program (Klein et al., 2014; see Supplemental Experimental Procedures). These data confirm that intact OCT4/SOX2 binding sites are necessary for inter-chromosomal contacts at the Oct4 locus during ESC differentiation.

Having confirmed inter-chromosomal contact between the WT *Oct4* locus and the *OCF2ΔYY1* locus at the molecular level, we next sought to assess whether loss of inter-chromosomal pairing would affect regulation at the *Oct4* locus. Previous studies have shown that the methyltransferase G9A is targeted

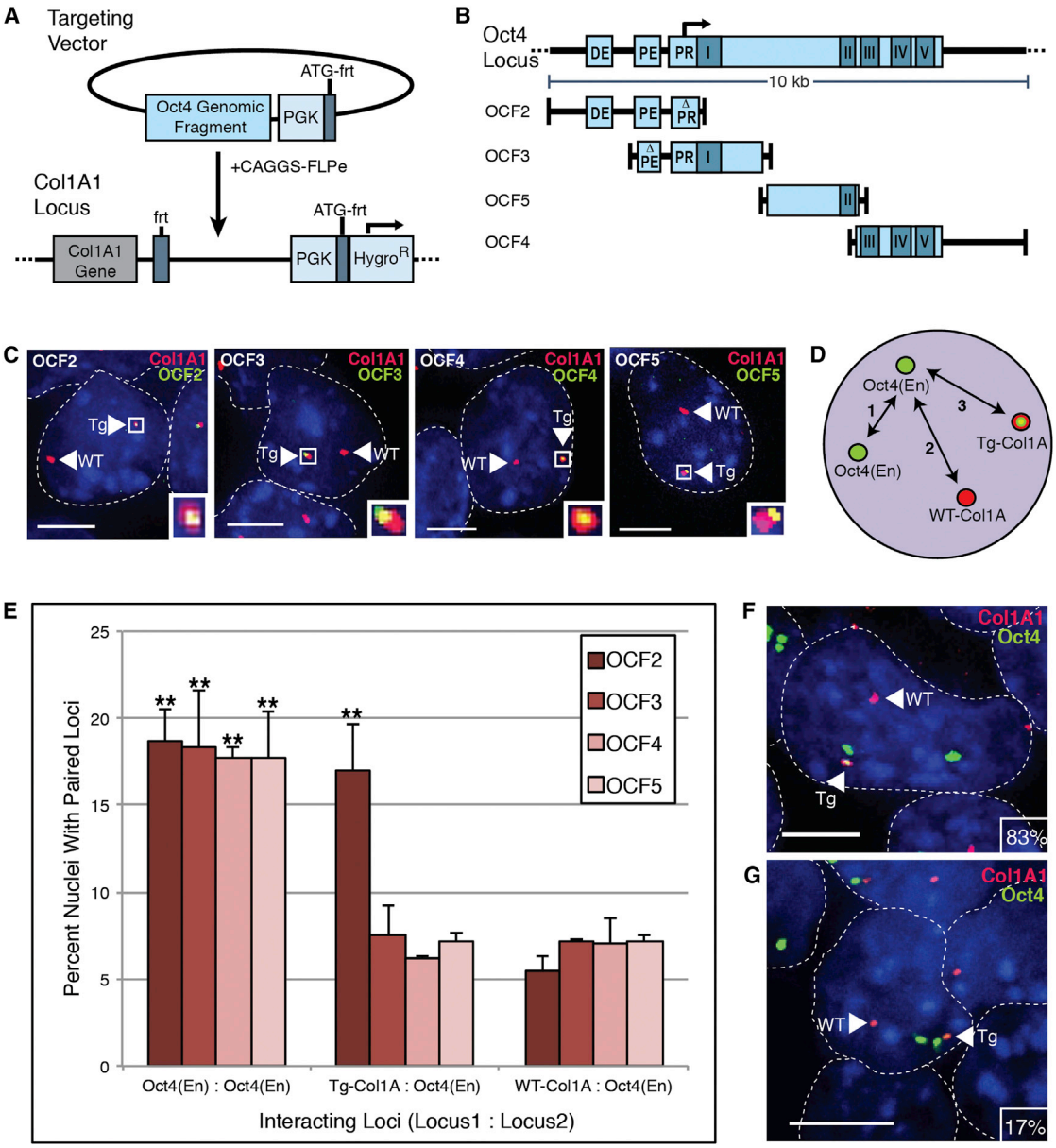

Figure 4. A DNA Fragment Encompassing the 5′ Regulatory Region of the *Oct4* Gene Is Sufficient to Induce Pairing with Endogenous *Oct4* Loci

(A) Schematic representation of a 10 kb genomic region at the *Oct4* locus on mouse chromosome 17, which was divided into four separate genomic DNA fragments: OCF2, OCF3, OCF4, and OCF5.

(B) Oct4 genomic fragments were inserted at the *Col1A1* locus in KH2 ESCs.

(C) Targeted insertion of Oct4 fragments at the Col1A1 locus was verified by DNA FISH. Representative images of each cell line are shown, with the transgenic (Tg) and WT *Col1A1* loci labeled. Inset images show an enlarged region of the Tg-*Col1A1* locus. Scale bar represent 5 μm.

(D) Schematic representation of distance measurements made between the endogenous *Oct4* alleles (Oct4(En)), the WT-*Col1A1* allele, and the transgenic *Col1A1* allele (Tg-*Col1A1*).

(E) Quantification of allelic interactions among endogenous *Oct4* loci (Oct4(En)), WT-*Col1A1*, and Tg-*Col1A1* in each cell line. n = 100 each time point, error bars represent ± SEM of three biological replicates. The p values for the two-sample z-test statistic are reported. **$p < 0.01$.

(F and G) Representative images of paired loci in OCF2 ESCs. Pairing of Tg-*Col1A* with (F) one endogenous *Oct4* locus was observed more frequently than simultaneous pairing of Tg-*Col1A* with both endogenous *Oct4* loci (G). Scale bar represents 5 μm.

See also Figure S4.

to the Oct4 locus during ESC differentiation, leading to an increase in di-methylation of Histone 3 Lysine 9 (H3K9me2) at the *Oct4* locus by day 5.5 (−)LIF (Feldman et al., 2006; Yamamizu et al., 2012). Evidence also indicates that G9A activity is necessary for stable repression and heterochromatinization of *Oct4* (Epsztejn-Litman et al., 2008; Feldman et al., 2006), making the

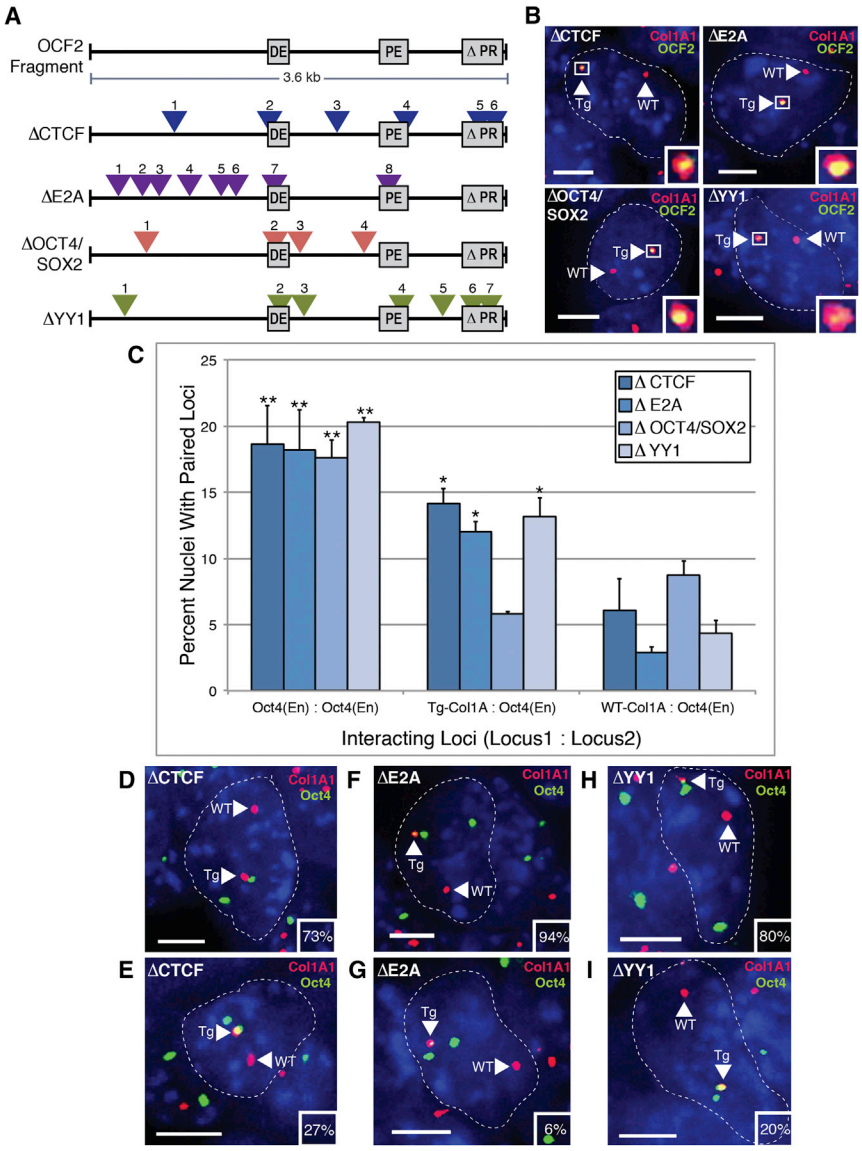

Figure 5. Mutation of Putative OCT4/SOX2 Binding Sites within the OCF2 DNA Fragment Abolishes Pairing with Endogenous *Oct4* Loci

(A) Schematic representation of the 3.6 kb OCF2 fragment, with putative binding sites for CTCF, E2A, OCT4/SOX2, and YY1.

(B) Targeted insertion of mutated OCF2 fragments at the *Col1A1* locus was verified by DNA FISH. Representative images of each cell line, with the transgenic (Tg) and WT *Col1A1* loci labeled. Inset images show enlarged region of the Tg-*Col1A1* locus. Scale bar represents 5 μm.

(C) Quantification of allelic interactions between endogenous *Oct4* loci (*Oct4(En)*), WT-*Col1A1*, and Tg-*Col1A1* in each cell line. n = 100 for each time point, error bars represent ± SEM of three biological replicates. The p values for the two-sample z-test statistic are reported. $^{**}p < 0.01$, $^{*}p < 0.05$.

(D–I) Representative images of paired loci in OCF2ΔCTCF, OCF2ΔYY1, and OCF2ΔE2A ESCs. Percentage of pairing events in each cell line involving two or three loci are indicated. Scale bar represents 5 μm.

See also Figure S5 and Table S3.

H3K9me2 modification a robust indicator of gene repression at the Oct4 locus. Thus, H3K9me2 ChIP was performed during ESC differentiation in pairing-deficient OCF2ΔOCT4/SOX2 ESCs and pairing-competent OCF2ΔYY1 ESCs to investigate the acquisition of this epigenetic mark at the WT and transgenic *Oct4* alleles during differentiation. H3K9me2 enrichment was assayed by qPCR at 0, 3, and 6 days (−)LIF, using allele-specific Taqman probes to distinguish between WT and transgenic *Oct4* alleles. As shown in Figure 7D, the pairing-deficient *OCF2ΔOCT4/SOX2* allele shows a significantly lower level of H3K9me2 enrichment by Day 6 (−)LIF compared to the WT *Oct4* allele at the same time point, indicating that the mutated locus is not regulated by the same mechanism as the WT *Oct4* locus. In contrast, the pairing-competent *OCF2ΔYY1* allele acquires the H3K9me2 marks with the same kinetics as the WT *Oct4* allele at all points examined during differentiation (Figure 7E), indicating that the transgenic *OCF2ΔYY1* allele, which is able to physically interact with WT *Oct4* alleles in *trans*, acquires the proper epigenetic marks in synchrony with WT *Oct4* alleles during ESC differentiation. Together, these data suggest that the loss of OCT4/SOX2 binding sites at the *Oct4* locus not only disrupts allelic pairing, but also affects accumulation of the repressive H3K9me2 modification at the *Oct4* enhancer region.

DISCUSSION

Thus far, studies that have addressed the relationship between gene position and transcriptional regulation have been performed in ESCs before the cells loose pluripotency, and then in differentiated cell populations after the cells have committed to a particular lineage (Aoto et al., 2006; Boyer et al., 2005; Jost et al., 2011; Loh et al., 2006; Mayer et al., 2005; Mikkelsen et al., 2007; Parada et al., 2004; Peric-Hupkes et al., 2010). Certainly, such studies have yielded important insights into the epigenetic and transcriptional differences between pluripotent and committed cell types. However, without examining the early intermediate steps between pluripotency and lineage commitment, it is impossible to understand how these differences are established. Herein, we have provided evidence of transient *Oct4* allelic pairing during the transition from pluripotency to lineage commitment during ESC differentiation, and importantly, also during embryonic development. Our data suggest that homologous pairing of *Oct4* alleles is correlated with the kinetics of ESC differentiation. Furthermore, we have identified DNA elements within the *Oct4* gene locus that mediate the allelic pairing event, and modulate the synchronous acquisition of repressive epigenetic marks during ESC differentiation.

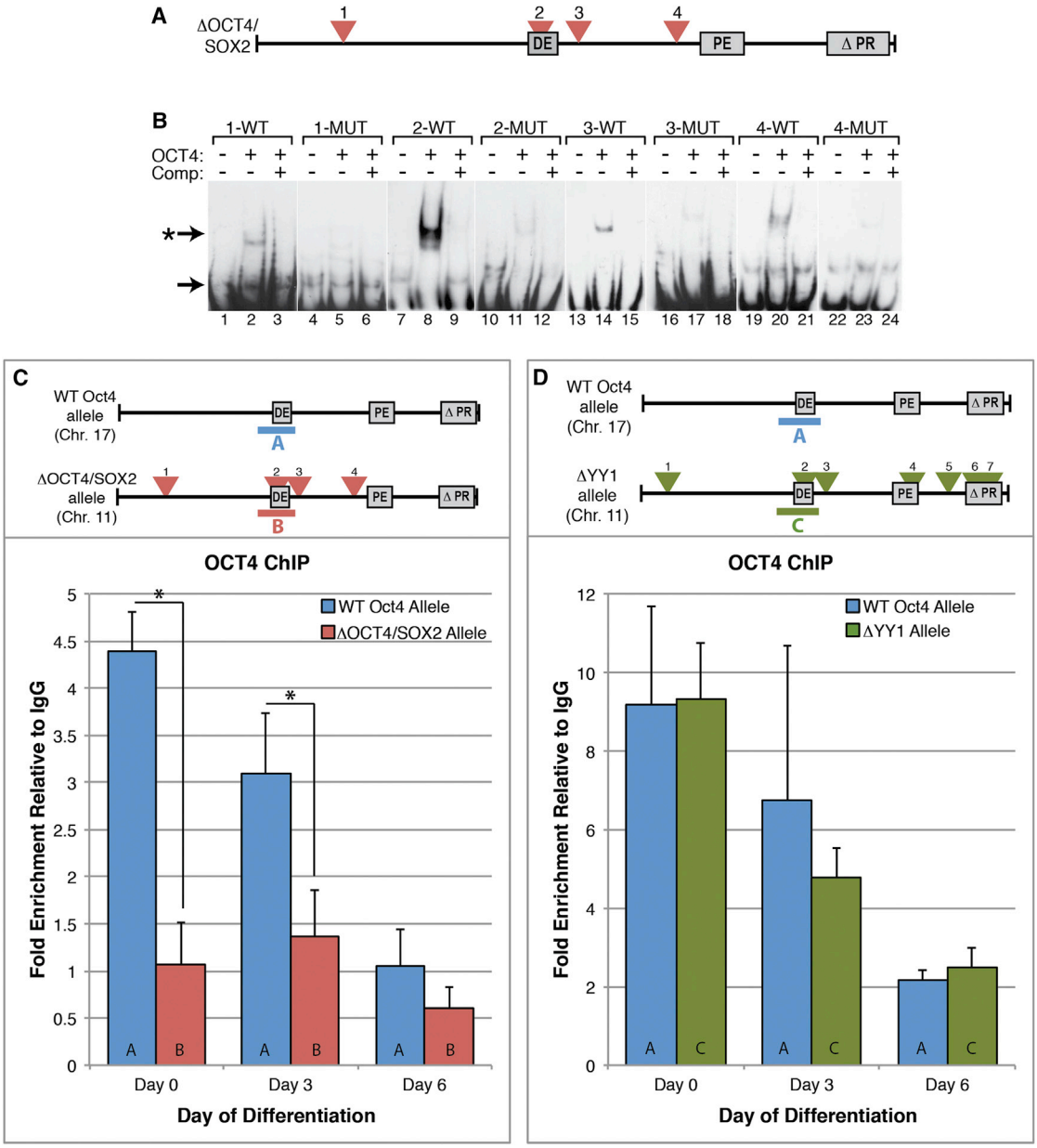

Figure 6. OCT4 Protein Binding at Four Sites within the OCF2 DNA Fragment Is Disrupted by Site-Directed Mutagenesis

(A) Schematic representation of the 3.6 kb OCF2 fragment, with putative binding sites for OCT4/SOX2 proteins indicated.

(B) Binding of recombinant OCT4 protein to WT or mutated oligos was assessed. Upward shift in the gel band (*→) indicates OCT4 binding. Unbound oligonucleotides are seen as a lower band (→).

(C) Oct4 ChIP-qPCR was performed in OCF2ΔOCT4/SOX2 ESCs differentiated for 0, 3, or 6 days (−)LIF. Allele-specific Taqman probes were used to distinguish the endogenous Oct4 distal enhancer (DE) region (chromosome [Chr.] 17, blue underline "A") from the mutated transgenic DE region (Chr. 11, red underline "B"). OCT4 enrichment at each site is reported relative to IgG. Error bars represent ± SEM of three biological replicates, and p values for Student's t-test are reported. *$p < 0.05$.

(D) Oct4 ChIP-qPCR was performed in OCF2ΔYY1 ESCs, using allele-specific Taqman probes to distinguish endogenous Oct4 distal enhancer (DE) region (Chr. 17, blue underline "A") from mutated transgenic DE region (Chr. 11, green underline "C"). OCT4 enrichment expressed relative to IgG. Error bars represent ± SEM of three biological replicates.

See also Table S4.

Our single-cell analyses extend several recent genome-wide studies, which find that genomic regions occupied by pluripotency factors such as OCT4, SOX2, and NANOG interact with each other at increased frequency, creating an ESC-specific chromatin organization profile (de Wit et al., 2013; Denholtz et al., 2013; Wei et al., 2013). In addition, our findings support

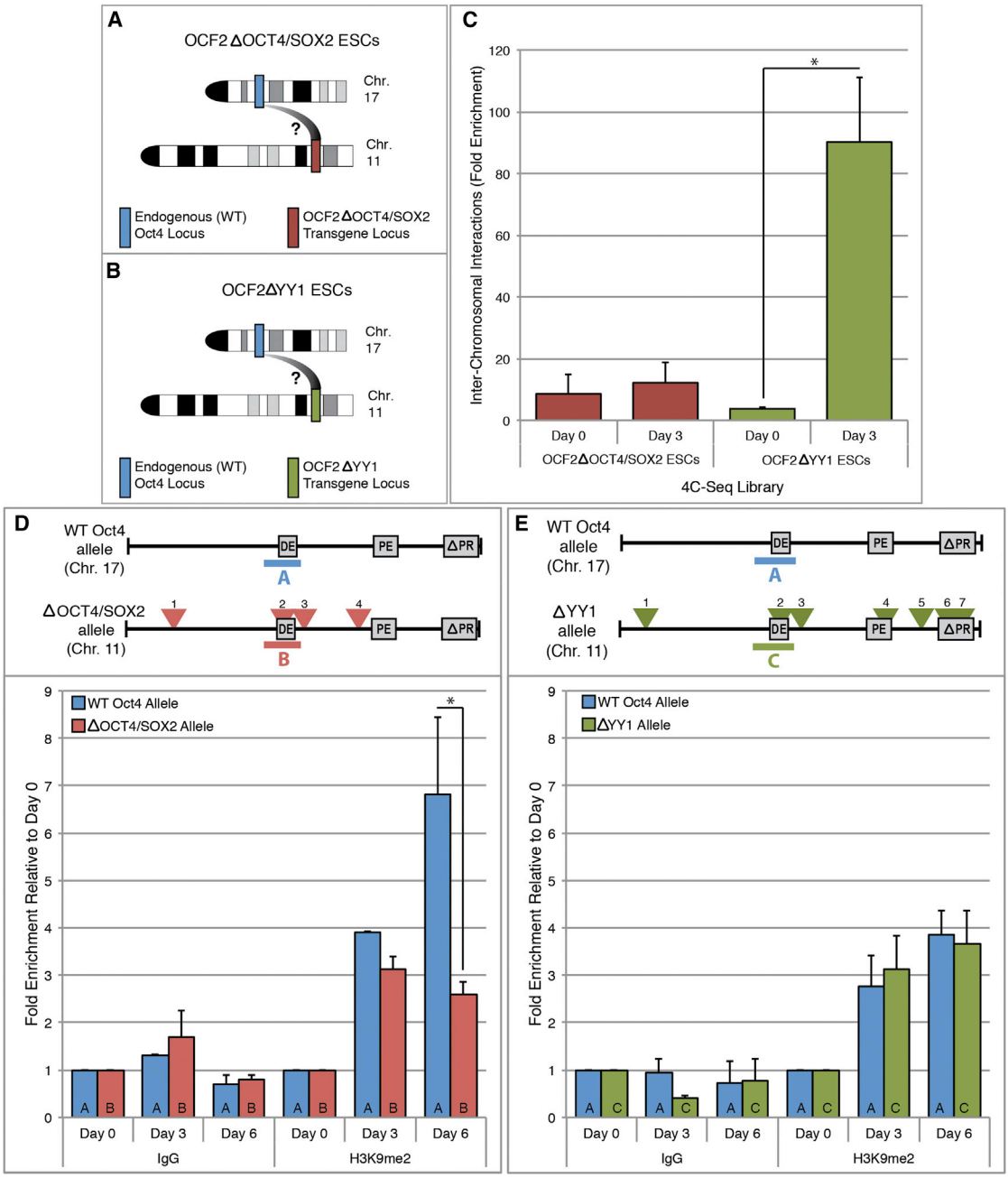

Figure 7. Intact OCT4/SOX2 Protein Binding Sites Are Necessary for Inter-Chromosomal Interactions in *Trans*

(A–C) Circular chromosome conformation capture followed by paired-end DNA sequencing (4C-seq) used to evaluate inter-chromosomal interactions between the WT endogenous Oct4 locus (Chr. 17) and a mutated OCF2 transgenic locus (Chr. 11) in (A) "pairing deficient" OCF2ΔOCT4/SOX2 ESCs and (B) "pairing competent" OCF2ΔYY1 ESCs. (C) The frequency of inter-chromosomal contacts between the WT Oct4 locus (Chr. 17) and a mutated OCF2 transgenic locus (Chr. 11) was determined and is reported as the fold enrichment relative to the background level of inter-chromosomal interactions at a non-interacting genomic region. The change in *trans*-interactions was compared between Day 0 and Day 3 in each cell line. Error bars represent ± SEM of two biological replicates, and p values for Student's t-test are reported. *$p < 0.05$.

(D) H3K9me2 ChIP-qPCR was performed in OCF2ΔOCT4/SOX2 ESCs differentiated for 0, 3, or 6 days (−)LIF. Allele-specific Taqman probes were used to distinguish the endogenous Oct4 distal enhancer (DE) region (Chr. 17, blue underline "A") from the mutated transgenic DE region (Chr. 11, red underline "B"). H3K9me2 enrichment at each site is reported as fold enrichment relative to Day 0 values. Error bars represent ± SEM of at least two biological replicates, and p values for Student's t-test are reported. *$p < 0.05$.

(E) H3K9me2 ChIP-qPCR was performed in OCF2ΔYY1 ESCs differentiated for 0, 3, or 6 days (−)LIF. Allele-specific Taqman probes were used to distinguish the WT Oct4 distal enhancer (DE) region (Chr. 17, blue underline "A") from the mutated transgenic DE region (Chr. 11, green underline "B"). H3K9me2 enrichment at each site is reported as fold enrichment relative to Day 0 values. Error bars represent ± SEM of at least two biological replicates.

a growing body of evidence that suggest a role for DNA elements bound by transcriptional activators/repressors in mediating chromatin organization in various organismal contexts (Apostolou et al., 2013; Babu et al., 2008; Bantignies et al., 2011; Brickner et al., 2012; Bulut-Karslioglu et al., 2012; Jing et al., 2008; Wei et al., 2013; Whyte et al., 2013).

Inter-chromosomal associations could be mediated through a variety of mechanisms. In the case of the *Oct4* gene locus, we identified the 5′ regulatory region of the *Oct4* gene (the OCF2 transgene fragment) as essential for mediating *Oct4* allelic pairing. Furthermore, we present evidence that four OCT4/SOX2 binding sites within this region are necessary for mediating inter-allelic associations. These findings imply that the OCT4 and/or SOX2 proteins, or other proteins that competitively bind to these DNA elements, mediate the observed *Oct4* allelic associations during ESC differentiation. Interestingly, the OCT4 protein has also been identified as a critical mediator of inter-chromosomal XIC associations during X chromosome inactivation (Donohoe et al., 2009). In addition, Oct4/Sox2 motifs have been identified in the imprinting control region (ICR) of the *H19/Igf2* locus (Hori et al., 2012), another genomic locus that has been shown to participate in functional inter-chromosomal interactions (Ling et al., 2006; Sandhu et al., 2009). Indeed, evidence suggests that the intact Oct4/Sox2 motif is necessary for proper DNA demethylation at the maternal ICR in both mouse and human cells (Abi Habib et al., 2014; Hori et al., 2012; Zimmerman et al., 2013). Together with our data, these studies suggest an important role for Oct4/Sox2 binding motifs at several genomic loci that participate in inter-chromosomal interactions, and that loss of these binding motifs can lead to epigenetic misregulation.

Although our findings clearly demonstrate that the OCT4 protein binds the Oct4/Sox2 elements in the OCF2 fragment in vitro and in vivo (Figure 6) and that the binding is essential for allelic pairing, we cannot rule out the possibility that additional proteins may bind these Oct4/Sox2 elements with OCT4 in an in vivo context. For instance, it has been reported that OCT4 can bind to these elements with SOX4, SOX11, SOX 14, SOX15, SOX17, or SOX21 instead of SOX2 (Masui et al., 2007). Similarly, SOX2 may bind enhancer elements with the POU family member BRN2 instead of OCT4 in some cell types (Lodato et al., 2013). In addition, the OCT4 protein has been shown to interact with various other proteins, including nucleosome remodelers, chromatin modifiers, Cohesin, Mediator, as well as proteins involved in nucleotide excision repair (Ding et al., 2012; Esch et al., 2013; Fong et al., 2011; Kagey et al., 2010; van den Berg et al., 2010). Thus, the flexibility of both OCT4 and SOX2 proteins to bind Oct4/Sox2 DNA elements with varied binding partners could allow these DNA elements to be utilized differently depending on the availability of protein binding partners in different cell types. Identification of proteins in addition to OCT4 that bind to these Oct4/Sox2 elements to mediate inter-chromosomal contacts will be the subject of future studies, and will extend our understanding of the impact of nuclear dynamics on transcriptional programs, and vice versa.

Unlike other described cases of homologous allelic associations in mammalian cells (Bacher et al., 2006; Hewitt et al., 2009; Krueger et al., 2012; LaSalle and Lalande, 1996; Thatcher et al., 2005), the *Oct4* gene is not imprinted and does not appear to be monoallelically expressed; therefore, *Oct4* allelic pairing is not likely to function in allelic exclusion. In *Drosophila*, where somatic homolog pairing is frequently observed, the term transvection is used to describe cases in which gene activity is influenced by the action of enhancers in *trans* (reviewed in Duncan, 2002). Although transvection has been studied most extensively in *Drosophila*, several studies suggest that homologous and heterologous alleles may also have the potential for *trans*-regulation in mammalian somatic cells (Krueger et al., 2012; Sandhu et al., 2009; Spilianakis et al., 2005; Yan et al., 2007). Given that the present study reveals an interaction between *Oct4* enhancer regions, our data are most consistent with transvection-like regulation at the *Oct4* locus.

Collectively, our results indicate that the dynamic reorganization of nuclear architecture that occurs during ESC differentiation, including *Oct4* allelic pairing, is likely linked to the changing transcriptional program in these cells. In the future, the development of live-cell imaging approaches to simultaneously depict *Oct4* gene position and transcription in ESCs and embryos will help to further elucidate the relationship between inter-chromosomal interactions and the transcriptional program during commitment and development.

EXPERIMENTAL PROCEDURES

ESC Lines

ESC lines containing transgenic single-copy insertions of Oct4 gene fragments were constructed by FLP recombination using the KH2 ESC line (Beard et al., 2006).

Oct4.468/R26-rtTA (Premsrirut et al., 2011) and KH2 ESC lines were kindly provided by S. Lowe, Memorial Sloan Kettering Cancer Center; and the v6.5 ESC line was provided by S. Kim, Cold Spring Harbor Laboratory. See also Table S2.

ESC Culture and Differentiation

Routine growth and maintenance of ESCs was carried out as previously described (Eckersley-Maslin et al., 2014), except that Oct4.468/R26-rtTA ESCs were cultured in ESC medium made with Tet System Approved Fetal Bovine Serum (Clontech).

ESCs were differentiated using either: (1) (−)LIF differentiation medium: DMEM high glucose (Invitrogen) containing 15% fetal bovine serum (FBS) (Invitrogen), 1× MEM-NEAA (Invitrogen), 0.1 U/ml pen/strep, and 2 μM 2-mercaptoethanol (Sigma). (2) RA differentiation medium: (−)LIF differentiation medium, plus 100 nM all-*trans* retinoic acid (Sigma). (3) DOX differentiation medium: (−)LIF differentiation medium, plus 1 μg/ml doxycycline (Sigma).

Mouse Embryo Collection, Fixation, and Cryosectioning

WT C57BL/6J embryos were recovered at 6.5, 7.75, and 9.5 days post-coitum (dpc). E6.5 embryos in utero were fixed in 4% paraformaldehyde (PFA) overnight at 4°C, E7.75 embryos were fixed in 4% PFA for 30 min at 4°C, and E9.5 embryos were fixed in 2% PFA overnight at 4°C. Serial sagittal sections of 10 μm thickness were prepared using a Leica cryostat. E7.75 embryos were staged according to Downs and Davies (1993).

Immunofluorescence and RNA and DNA FISH

Immunofluorescence, RNA FISH, and DNA FISH were performed as previously described (Eckersley-Maslin et al., 2014). For immunofluorescence, primary antibodies used included rabbit anti-Oct4 (H134, Santa-Cruz, 1:200) and rabbit anti-LaminB1 (Abcam, 1:500). Detailed protocol is available in the Supplemental Experimental Procedures.

Multi-Site-Directed Mutagenesis of pOCF2

Putative binding sites for the candidate proteins were identified in the OCF2 DNA sequence using the MatInspector program (Genomatix Software, Table S3). Putative binding sites were scrambled using Sequence Scrambler (http://molbiol.ru/eng/scripts/01_16.html) and primers were designed (Table S3) for

use with the QuikChange Lightening Multi-Site-Directed Mutagenesis Kit (Agilent). Mutagenesis was performed according to the manufacturer's protocol, and the sequences of the resulting plasmids were verified by DNA sequencing.

Microscopy and Image Analysis

Image acquisition was carried out on an Applied Precision DeltaVision Core microscope with a PlanApo 60 × 1.40 numerical aperture objective lens (Olympus America); 50–150 image stacks (200 nm thickness) were acquired of each ESC colony, depending on the thickness of the ESC colony in each instance. Acquired images were subsequently deconvolved and analyzed using SoftWoRx Suite 2.0 software (Applied Precision). Cell nuclei were manually segmented, and distances between DNA FISH signals in the acquired, deconvolved images were measured in 3D. The distance between two points was measured as the distance from the center of one fluorescent signal to the other. In each experiment, only nuclei with two or four visible fluorescent signals for each locus were included in the analysis.

Statistical Analysis of Allelic Pairing Frequencies

The distribution of heterologous distances between non-co-regulated genes was used to calculate the expected frequency of random inter-allelic associations at each time point (Figure S1), as previously described (LaSalle and Lalande, 1996).

The two-sample z-test statistic was used to assess whether the observed frequency of allelic pairing events was more than the expected frequency of random inter-allelic associations (Figure S1). A $p < 0.05$ was considered significant, and sufficient to reject the null hypothesis.

4C Template Preparation, Paired-End Sequencing, and Data Analysis

4C templates for OCF2ΔOCT4/SOX2 and OCF2ΔYY1 ESCs at Day 0 and Day 3 (−)LIF were prepared as previously described (Splinter et al., 2012), and sequences were amplified from the 4C template using primers for the OCF2 and control (154.9) viewpoints. Pooled libraries were sequenced on an Illumina MiSeq PE300. Obtained reads were separated using custom perl scripts based on the sample, genotyping SNPs, and/or the presence of sequences unique to the WT *Oct4*, *OCF2ΔOctSox* and *OCF2ΔYY1* loci. Intra-chromosomal interactions were assessed using the FourCSeq program (Klein et al., 2014). Inter-chromosomal interaction frequencies are expressed as a fold difference from the average inter-chromosomal interaction frequencies observed at the control (154.9) viewpoint. A detailed protocol is provided in the Supplemental Experimental Procedures.

Allele-Specific ChIP-qPCR

ChIP for OCT4 and H3K9me was performed in OCF2ΔOCT4/SOX2 and OCF2-ΔYY1 ESCs at Day 0, Day 3, and Day 6 (−)LIF, using methods described previously (Marson et al., 2008). For qPCR, allele-specific Taqman probes with distinct reporters were used simultaneously in each PCR reaction to distinguish between occupancy at the endogenous Oct4 DE on chromosome 17 and the mutated transgenic Oct4 DE region on chromosome 11 (see the Supplemental Experimental Procedures). For OCT4 ChIP, enrichment at each site is reported as fold-change relative to IgG in each biological replicate. For H3K9me2 ChIP, a standard curve was first used to determine the quantity of DNA pulled down in each sample, and then the quantity normalized relative to the starting amount at Day 0 for each biological replicate. H3K9me2 enrichment is then expressed as the fold-change from Day 0 at each time point and compared to IgG.

ACCESSION NUMBERS

The NCBI Gene Expression Omnibus accession number for the PE-4Cseq data sets reported in this paper is GSE65510.

SUPPLEMENTAL INFORMATION

Supplemental Information includes Supplemental Experimental Procedures, five figures, and four tables and can be found with this article online at http://dx.doi.org/10.1016/j.stem.2015.02.001.

ACKNOWLEDGMENTS

We thank Edith Heard, Alea Mills, Jane Skok, Mona Spector, Bruce Stillman, and all members of the Spector Laboratory for helpful discussions and suggestions. We also thank Sang-Yong Kim and Scott Lowe for providing ESC lines used in this study. We gratefully acknowledge the CSHL Microscopy Shared Resource for assistance with microscopic imaging and the CSHL Histology Shared Resource for assistance with cryosections (NCI 2P3OCA45508). M.S.H. was supported by The Watson School of Biological Sciences and the Starr Foundation. This research was supported by GM42694 (to D.L.S.) and CA121852 (to M.M.S.).

Received: October 25, 2013
Revised: December 3, 2014
Accepted: February 2, 2015
Published: March 5, 2015

REFERENCES

Abi Habib, W., Azzi, S., Brioude, F., Steunou, V., Thibaud, N., Das Neves, C., Le Jule, M., Chantot-Bastaraud, S., Keren, B., Lyonnet, S., et al. (2014). Extensive investigation of the IGF2/H19 imprinting control region reveals novel OCT4/SOX2 binding site defects associated with specific methylation patterns in Beckwith-Wiedemann syndrome. Hum. Mol. Genet. *23*, 5763–5773.

Aoto, T., Saitoh, N., Ichimura, T., Niwa, H., and Nakao, M. (2006). Nuclear and chromatin reorganization in the MHC-Oct3/4 locus at developmental phases of embryonic stem cell differentiation. Dev. Biol. *298*, 354–367.

Apostolou, E., Ferrari, F., Walsh, R.M., Bar-Nur, O., Stadtfeld, M., Cheloufi, S., Stuart, H.T., Polo, J.M., Ohsumi, T.K., Borowsky, M.L., et al. (2013). Genome-wide chromatin interactions of the Nanog locus in pluripotency, differentiation, and reprogramming. Cell Stem Cell *12*, 699–712.

Augui, S., Filion, G.J., Huart, S., Nora, E., Guggiari, M., Maresca, M., Stewart, A.F., and Heard, E. (2007). Sensing X chromosome pairs before X inactivation via a novel X-pairing region of the Xic. Science *318*, 1632–1636.

Babu, D.A., Chakrabarti, S.K., Garmey, J.C., and Mirmira, R.G. (2008). Pdx1 and BETA2/NeuroD1 participate in a transcriptional complex that mediates short-range DNA looping at the insulin gene. J. Biol. Chem. *283*, 8164–8172.

Bacher, C.P., Guggiari, M., Brors, B., Augui, S., Clerc, P., Avner, P., Eils, R., and Heard, E. (2006). Transient colocalization of X-inactivation centres accompanies the initiation of X inactivation. Nat. Cell Biol. *8*, 293–299.

Bantignies, F., Roure, V., Comet, I., Leblanc, B., Schuettengruber, B., Bonnet, J., Tixier, V., Mas, A., and Cavalli, G. (2011). Polycomb-dependent regulatory contacts between distant Hox loci in Drosophila. Cell *144*, 214–226.

Beard, C., Hochedlinger, K., Plath, K., Wutz, A., and Jaenisch, R. (2006). Efficient method to generate single-copy transgenic mice by site-specific integration in embryonic stem cells. Genesis *44*, 23–28.

Boyer, L.A., Lee, T.I., Cole, M.F., Johnstone, S.E., Levine, S.S., Zucker, J.P., Guenther, M.G., Kumar, R.M., Murray, H.L., Jenner, R.G., et al. (2005). Core transcriptional regulatory circuitry in human embryonic stem cells. Cell *122*, 947–956.

Brickner, D.G., Ahmed, S., Meldi, L., Thompson, A., Light, W., Young, M., Hickman, T.L., Chu, F., Fabre, E., and Brickner, J.H. (2012). Transcription factor binding to a DNA zip code controls interchromosomal clustering at the nuclear periphery. Dev. Cell *22*, 1234–1246.

Brown, J.M., Green, J., das Neves, R.P., Wallace, H.A., Smith, A.J., Hughes, J., Gray, N., Taylor, S., Wood, W.G., Higgs, D.R., et al. (2008). Association between active genes occurs at nuclear speckles and is modulated by chromatin environment. J. Cell Biol. *182*, 1083–1097.

Bulut-Karslioglu, A., Perrera, V., Scaranaro, M., de la Rosa-Velazquez, I.A., van de Nobelen, S., Shukeir, N., Popow, J., Gerle, B., Opravil, S., Pagani, M., et al. (2012). A transcription factor-based mechanism for mouse heterochromatin formation. Nat. Struct. Mol. Biol. *19*, 1023–1030.

Chaumeil, J., and Skok, J.A. (2012). The role of CTCF in regulating V(D)J recombination. Curr. Opin. Immunol. *24*, 153–159.

de Wit, E., Bouwman, B.A.M., Zhu, Y., Klous, P., Splinter, E., Verstegen, M.J.A.M., Krijger, P.H.L., Festuccia, N., Nora, E.P., Welling, M., et al. (2013). The pluripotent genome in three dimensions is shaped around pluripotency factors. Nature *501*, 227–231.

Denholtz, M., Bonora, G., Chronis, C., Splinter, E., de Laat, W., Ernst, J., Pellegrini, M., and Plath, K. (2013). Long-range chromatin contacts in embryonic stem cells reveal a role for pluripotency factors and polycomb proteins in genome organization. Cell Stem Cell *13*, 602–616.

Ding, J., Xu, H., Faiola, F., Ma'ayan, A., and Wang, J. (2012). Oct4 links multiple epigenetic pathways to the pluripotency network. Cell Res. *22*, 155–167.

Dixon, J.R., Selvaraj, S., Yue, F., Kim, A., Li, Y., Shen, Y., Hu, M., Liu, J.S., and Ren, B. (2012). Topological domains in mammalian genomes identified by analysis of chromatin interactions. Nature *485*, 376–380.

Donohoe, M.E., Silva, S.S., Pinter, S.F., Xu, N., and Lee, J.T. (2009). The pluripotency factor Oct4 interacts with Ctcf and also controls X-chromosome pairing and counting. Nature *460*, 128–132.

Downs, K.M. (2008). Systematic localization of Oct-3/4 to the gastrulating mouse conceptus suggests manifold roles in mammalian development. Dev. Dyn. *237*, 464–475.

Downs, K.M., and Davies, T. (1993). Staging of gastrulating mouse embryos by morphological landmarks in the dissecting microscope. Development *118*, 1255–1266.

Duan, Z., and Blau, C.A. (2012). The genome in space and time: does form always follow function? How does the spatial and temporal organization of a eukaryotic genome reflect and influence its functions? BioEssays *34*, 800–810.

Duncan, I.W. (2002). Transvection effects in Drosophila. Annu. Rev. Genet. *36*, 521–556.

Ebert, A., McManus, S., Tagoh, H., Medvedovic, J., Salvagiotto, G., Novatchkova, M., Tamir, I., Sommer, A., Jaritz, M., and Busslinger, M. (2011). The distal V(H) gene cluster of the Igh locus contains distinct regulatory elements with Pax5 transcription factor-dependent activity in pro-B cells. Immunity *34*, 175–187.

Eckersley-Maslin, M.A., Bergmann, J.H., Lazar, Z., and Spector, D.L. (2013). Lamin A/C is expressed in pluripotent mouse embryonic stem cells. Nucleus *4*, 53–60.

Eckersley-Maslin, M.A., Thybert, D., Bergmann, J.H., Marioni, J.C., Flicek, P., and Spector, D.L. (2014). Random monoallelic gene expression increases upon embryonic stem cell differentiation. Dev. Cell *28*, 351–365.

Epsztejn-Litman, S., Feldman, N., Abu-Remaileh, M., Shufaro, Y., Gerson, A., Ueda, J., Deplus, R., Fuks, F., Shinkai, Y., Cedar, H., and Bergman, Y. (2008). De novo DNA methylation promoted by G9a prevents reprogramming of embryonically silenced genes. Nat. Struct. Mol. Biol. *15*, 1176–1183.

Esch, D., Vahokoski, J., Groves, M.R., Pogenberg, V., Cojocaru, V., Vom Bruch, H., Han, D., Drexler, H.C., Araúzo-Bravo, M.J., Ng, C.K., et al. (2013). A unique Oct4 interface is crucial for reprogramming to pluripotency. Nat. Cell Biol. *15*, 295–301.

Feldman, N., Gerson, A., Fang, J., Li, E., Zhang, Y., Shinkai, Y., Cedar, H., and Bergman, Y. (2006). G9a-mediated irreversible epigenetic inactivation of Oct-3/4 during early embryogenesis. Nat. Cell Biol. *8*, 188–194.

Fong, Y.W., Inouye, C., Yamaguchi, T., Cattoglio, C., Grubisic, I., and Tjian, R. (2011). A DNA repair complex functions as an Oct4/Sox2 coactivator in embryonic stem cells. Cell *147*, 120–131.

Hewitt, S.L., Yin, B., Ji, Y., Chaumeil, J., Marszalek, K., Tenthorey, J., Salvagiotto, G., Steinel, N., Ramsey, L.B., Ghysdael, J., et al. (2009). RAG-1 and ATM coordinate monoallelic recombination and nuclear positioning of immunoglobulin loci. Nat. Immunol. *10*, 655–664.

Hori, N., Yamane, M., Kouno, K., and Sato, K. (2012). Induction of DNA demethylation depending on two sets of Sox2 and adjacent Oct3/4 binding sites (Sox-Oct motifs) within the mouse H19/insulin-like growth factor 2 (Igf2) imprinted control region. J. Biol. Chem. *287*, 44006–44016.

Hübner, M.R., Eckersley-Maslin, M.A., and Spector, D.L. (2013). Chromatin organization and transcriptional regulation. Curr. Opin. Genet. Dev. *23*, 89–95.

Jing, H., Vakoc, C.R., Ying, L., Mandat, S., Wang, H., Zheng, X., and Blobel, G.A. (2008). Exchange of GATA factors mediates transitions in looped chromatin organization at a developmentally regulated gene locus. Mol. Cell *29*, 232–242.

Joffe, B., Leonhardt, H., and Solovei, I. (2010). Differentiation and large scale spatial organization of the genome. Curr. Opin. Genet. Dev. *20*, 562–569.

Jost, K.L., Haase, S., Smeets, D., Schrode, N., Schmiedel, J.M., Bertulat, B., Herzel, H., Cremer, M., and Cardoso, M.C. (2011). 3D-Image analysis platform monitoring relocation of pluripotency genes during reprogramming. Nucleic Acids Res. *39*, e113–e113.

Kagey, M.H., Newman, J.J., Bilodeau, S., Zhan, Y., Orlando, D.A., van Berkum, N.L., Ebmeier, C.C., Goossens, J., Rahl, P.B., Levine, S.S., et al. (2010). Mediator and cohesin connect gene expression and chromatin architecture. Nature *467*, 430–435.

Klein, F.A., Anders, S., Pakozdi, T., Ghavi-Helm, Y., Furlong, E.E.M., and Huber, W. (2014). FourCSeq: analysis of 4C sequencing data. bioRχiv. http://dx.doi.org/10.1101/009548.

Kobayakawa, S., Miike, K., Nakao, M., and Abe, K. (2007). Dynamic changes in the epigenomic state and nuclear organization of differentiating mouse embryonic stem cells. Genes Cells *12*, 447–460.

Kosak, S.T., Scalzo, D., Alworth, S.V., Li, F., Palmer, S., Enver, T., Lee, J.S.J., and Groudine, M. (2007). Coordinate gene regulation during hematopoiesis is related to genomic organization. PLoS Biol. *5*, e309.

Krueger, C., King, M.R., Krueger, F., Branco, M.R., Osborne, C.S., Niakan, K.K., Higgins, M.J., and Reik, W. (2012). Pairing of homologous regions in the mouse genome is associated with transcription but not imprinting status. PLoS ONE *7*, e38983.

LaSalle, J.M., and Lalande, M. (1996). Homologous association of oppositely imprinted chromosomal domains. Science *272*, 725–728.

Lieberman-Aiden, E., van Berkum, N.L., Williams, L., Imakaev, M., Ragoczy, T., Telling, A., Amit, I., Lajoie, B.R., Sabo, P.J., Dorschner, M.O., et al. (2009). Comprehensive mapping of long-range interactions reveals folding principles of the human genome. Science *326*, 289–293.

Ling, J.Q., Li, T., Hu, J.F., Vu, T.H., Chen, H.L., Qiu, X.W., Cherry, A.M., and Hoffman, A.R. (2006). CTCF mediates interchromosomal colocalization between Igf2/H19 and Wsb1/Nf1. Science *312*, 269–272.

Lodato, M.A., Ng, C.W., Wamstad, J.A., Cheng, A.W., Thai, K.K., Fraenkel, E., Jaenisch, R., and Boyer, L.A. (2013). SOX2 co-occupies distal enhancer elements with distinct POU factors in ESCs and NPCs to specify cell state. PLoS Genet. *9*, e1003288.

Loh, Y.-H., Wu, Q., Chew, J.-L., Vega, V.B., Zhang, W., Chen, X., Bourque, G., George, J., Leong, B., Liu, J., et al. (2006). The Oct4 and Nanog transcription network regulates pluripotency in mouse embryonic stem cells. Nat. Genet. *38*, 431–440.

Lupu, F., Alves, A., Anderson, K., Doye, V., and Lacy, E. (2008). Nuclear pore composition regulates neural stem/progenitor cell differentiation in the mouse embryo. Dev. Cell *14*, 831–842.

Marson, A., Levine, S.S., Cole, M.F., Frampton, G.M., Brambrink, T., Johnstone, S., Guenther, M.G., Johnston, W.K., Wernig, M., Newman, J., et al. (2008). Connecting microRNA genes to the core transcriptional regulatory circuitry of embryonic stem cells. Cell *134*, 521–533.

Masui, S., Nakatake, Y., Toyooka, Y., Shimosato, D., Yagi, R., Takahashi, K., Okochi, H., Okuda, A., Matoba, R., Sharov, A.A., et al. (2007). Pluripotency governed by Sox2 via regulation of Oct3/4 expression in mouse embryonic stem cells. Nat. Cell Biol. *9*, 625–635.

Masui, O., Bonnet, I., Le Baccon, P., Brito, I., Pollex, T., Murphy, N., Hupé, P., Barillot, E., Belmont, A.S., and Heard, E. (2011). Live-cell chromosome dynamics and outcome of X chromosome pairing events during ES cell differentiation. Cell *145*, 447–458.

Mayer, R., Brero, A., von Hase, J., Schroeder, T., Cremer, T., and Dietzel, S. (2005). Common themes and cell type specific variations of higher order chromatin arrangements in the mouse. BMC Cell Biol. *6*, 44.

Melcer, S., Hezroni, H., Rand, E., Nissim-Rafinia, M., Skoultchi, A., Stewart, C.L., Bustin, M., and Meshorer, E. (2012). Histone modifications and lamin A regulate chromatin protein dynamics in early embryonic stem cell differentiation. Nat. Commun. *3*, 910.

Meshorer, E., and Misteli, T. (2006). Chromatin in pluripotent embryonic stem cells and differentiation. Nat. Rev. Mol. Cell Biol. *7*, 540–546.

Mikkelsen, T.S., Ku, M., Jaffe, D.B., Issac, B., Lieberman, E., Giannoukos, G., Alvarez, P., Brockman, W., Kim, T.-K., Koche, R.P., et al. (2007). Genome-wide maps of chromatin state in pluripotent and lineage-committed cells. Nature *448*, 553–560.

Nagano, T., Lubling, Y., Stevens, T.J., Schoenfelder, S., Yaffe, E., Dean, W., Laue, E.D., Tanay, A., and Fraser, P. (2013). Single-cell Hi-C reveals cell-to-cell variability in chromosome structure. Nature *502*, 59–64.

Nora, E.P., Lajoie, B.R., Schulz, E.G., Giorgetti, L., Okamoto, I., Servant, N., Piolot, T., van Berkum, N.L., Meisig, J., Sedat, J., et al. (2012). Spatial partitioning of the regulatory landscape of the X-inactivation centre. Nature *485*, 381–385.

Osorno, R., Tsakiridis, A., Wong, F., Cambray, N., Economou, C., Wilkie, R., Blin, G., Scotting, P.J., Chambers, I., and Wilson, V. (2012). The developmental dismantling of pluripotency is reversed by ectopic Oct4 expression. Development *139*, 2288–2298.

Papantonis, A., Kohro, T., Baboo, S., Larkin, J.D., Deng, B., Short, P., Tsutsumi, S., Taylor, S., Kanki, Y., Kobayashi, M., et al. (2012). TNFα signals through specialized factories where responsive coding and miRNA genes are transcribed. EMBO J. *31*, 4404–4414.

Parada, L.A., McQueen, P.G., and Misteli, T. (2004). Tissue-specific spatial organization of genomes. Genome Biol. *5*, R44.

Peric-Hupkes, D., Meuleman, W., Pagie, L., Bruggeman, S.W.M., Solovei, I., Brugman, W., Gräf, S., Flicek, P., Kerkhoven, R.M., van Lohuizen, M., et al. (2010). Molecular maps of the reorganization of genome-nuclear lamina interactions during differentiation. Mol. Cell *38*, 603–613.

Phillips-Cremins, J.E., Sauria, M.E.G., Sanyal, A., Gerasimova, T.I., Lajoie, B.R., Bell, J.S.K., Ong, C.-T., Hookway, T.A., Guo, C., Sun, Y., et al. (2013). Architectural protein subclasses shape 3D organization of genomes during lineage commitment. Cell *153*, 1281–1295.

Premsrirut, P.K., Dow, L.E., Kim, S.Y., Camiolo, M., Malone, C.D., Miething, C., Scuoppo, C., Zuber, J., Dickins, R.A., Kogan, S.C., et al. (2011). A rapid and scalable system for studying gene function in mice using conditional RNA interference. Cell *145*, 145–158.

Sandhu, K.S., Shi, C., Sjölinder, M., Zhao, Z., Göndör, A., Liu, L., Tiwari, V.K., Guibert, S., Emilsson, L., Imreh, M.P., and Ohlsson, R. (2009). Nonallelic transvection of multiple imprinted loci is organized by the H19 imprinting control region during germline development. Genes Dev. *23*, 2598–2603.

Schoenfelder, S., Sexton, T., Chakalova, L., Cope, N.F., Horton, A., Andrews, S., Kurukuti, S., Mitchell, J.A., Umlauf, D., Dimitrova, D.S., et al. (2010). Preferential associations between co-regulated genes reveal a transcriptional interactome in erythroid cells. Nat. Genet. *42*, 53–61.

Simonis, M., Klous, P., Splinter, E., Moshkin, Y., Willemsen, R., de Wit, E., van Steensel, B., and de Laat, W. (2006). Nuclear organization of active and inactive chromatin domains uncovered by chromosome conformation capture-on-chip (4C). Nat. Genet. *38*, 1348–1354.

Spilianakis, C.G., Lalioti, M.D., Town, T., Lee, G.R., and Flavell, R.A. (2005). Interchromosomal associations between alternatively expressed loci. Nature *435*, 637–645.

Splinter, E., de Wit, E., van de Werken, H.J.G., Klous, P., and de Laat, W. (2012). Determining long-range chromatin interactions for selected genomic sites using 4C-seq technology: from fixation to computation. Methods *58*, 221–230.

Thatcher, K.N., Peddada, S., Yasui, D.H., and Lasalle, J.M. (2005). Homologous pairing of 15q11-13 imprinted domains in brain is developmentally regulated but deficient in Rett and autism samples. Hum. Mol. Genet. *14*, 785–797.

van den Berg, D.L.C., Snoek, T., Mullin, N.P., Yates, A., Bezstarosti, K., Demmers, J., Chambers, I., and Poot, R.A. (2010). An Oct4-centered protein interaction network in embryonic stem cells. Cell Stem Cell *6*, 369–381.

Wei, Z., Gao, F., Kim, S., Yang, H., Lyu, J., An, W., Wang, K., and Lu, W. (2013). Klf4 organizes long-range chromosomal interactions with the oct4 locus in reprogramming and pluripotency. Cell Stem Cell *13*, 36–47.

Whyte, W.A., Orlando, D.A., Hnisz, D., Abraham, B.J., Lin, C.Y., Kagey, M.H., Rahl, P.B., Lee, T.I., and Young, R.A. (2013). Master transcription factors and mediator establish super-enhancers at key cell identity genes. Cell *153*, 307–319.

Yamamizu, K., Fujihara, M., Tachibana, M., Katayama, S., Takahashi, A., Hara, E., Imai, H., Shinkai, Y., and Yamashita, J.K. (2012). Protein kinase A determines timing of early differentiation through epigenetic regulation with G9a. Cell Stem Cell *10*, 759–770.

Yan, J., Bi, W., and Lupski, J.R. (2007). Penetrance of craniofacial anomalies in mouse models of Smith-Magenis syndrome is modified by genomic sequence surrounding Rai1: not all null alleles are alike. Am. J. Hum. Genet. *80*, 518–525.

Young, R.A. (2011). Control of the embryonic stem cell state. Cell *144*, 940–954.

Zhang, Y., Wong, C.-H., Birnbaum, R.Y., Li, G., Favaro, R., Ngan, C.Y., Lim, J., Tai, E., Poh, H.M., Wong, E., et al. (2013). Chromatin connectivity maps reveal dynamic promoter-enhancer long-range associations. Nature *504*, 306–310.

Zimmerman, D.L., Boddy, C.S., and Schoenherr, C.S. (2013). Oct4/Sox2 binding sites contribute to maintaining hypomethylation of the maternal igf2/h19 imprinting control region. PLoS ONE *8*, e81962.